The Observation and Simulation of Diurnal Evaporation Contrast in an Alaskan Alpine Pass

ANTHONY JAMES BRAZEL

Dept. of Geography, University of Windsor, Ontario, Canada

SAMUEL I. OUTCALT

Dept. of Geography, University of Michigan, Ann Arbor

(Manuscript received 30 March 1973, in revised form 10 July 1973)

ABSTRACT

The surface climate simulation strategy developed by Myrup and modified by Outcalt was employed in the analysis of evaporation in rough alpine tundra terrain at Chitistone Pass, Alaska (61N, 142W, 1773 m MSL). The observations of evaporation for clear weather compare favorably with simulation estimates, especially for sites where water availability is not a limiting factor. Drier sites produce divergence between simulation and actual evaporation calculations. Further development is necessary to produce a working simulation model that incorporates both a water and heat budget synthesis for tundra terrain. However, with the employment of the equilibrium temperature model, the contrast of evaporation over tundra terrain appears to be predictable.

1. Introduction

Numerical models as tools in climatology can be extremely powerful, especially if verified for areas where even routine environmental monitoring is lacking. One example is the high alpine tundra, particularly the alpine pass. These areas channel human transportation and can represent important ecological niches for flora and fauna (Scott, 1971), and thus are deserving of scientific inquiry.

Knowledge of the microclimatic conditions, particularly the modeling of these conditions, is relevant in such locations and can aid in the spatial analysis of plant communities and geomorphic conditions in the alpine pass environment.

This paper describes a portion of an experiment which consisted of the observation and simulation of the energy transfer climatology of alpine pass terrain.

Observations were made which permitted simple energy balance calculations at locations with variable radiative, subsurface thermal, and topographic conditions. The energy balance simulation experiment made use of the model structure developed by Myrup (1969) and recently modified by Outcalt (1972a).

Observations were obtained by recording net radiation, subsurface heat flux, and gradients of dry and wet bulb temperatures. The Bowen ratio or energy balance approach was followed in the calculation of evaporation (Bowen, 1926). Rouse and Stewart (1972) followed a similar procedure for a tundra site in northern Ontario.

Specifically, this paper discusses the correlation between observations and model estimates of evaporation for sunny days at three specific sites at Chitistone Pass, Alaska. The pass site is located in the southeastern corner of Alaska between the Wrangell and St. Elias Mountains at approximately 1773 m MSL (see Figs. 1 and 2).

Simulated and observed evaporation rates are compared for sites 1, 4 and 5 (see Fig. 1). One of the assumptions in the model is that when the equilibrium temperature is specified, all generated energy budget components are appropriately correct in magnitude and direction. This assumption is tested here by analyzing evaporation.

Energy transfer simulations were developed by using the evolving strategy of synthetic climatological analysis (see e.g., Brunt, 1934; Lettau, 1951; Lonnqvist, 1962, 1963). More recently, Myrup (1969) and Outcalt (1972) have demonstrated the wide-ranging utility of the equilibrium temperature scheme. Brazel and Outcalt (1973) have discussed the power of this model for predicting the diurnal regime of surface temperature at the Chitistone Pass location. Fig. 3 shows the results of that study, and indicates strong correlations between model and observed estimates of surface and −10 cm temperatures for a clear day condition at the three sites studied in this paper. Two additional sites are shown, one on a flat surface, and the other on a southeast-facing slope (sites 2 and 3 respectively in Fig. 1). However, these sites are not analyzed here since evaporation observations are not available.

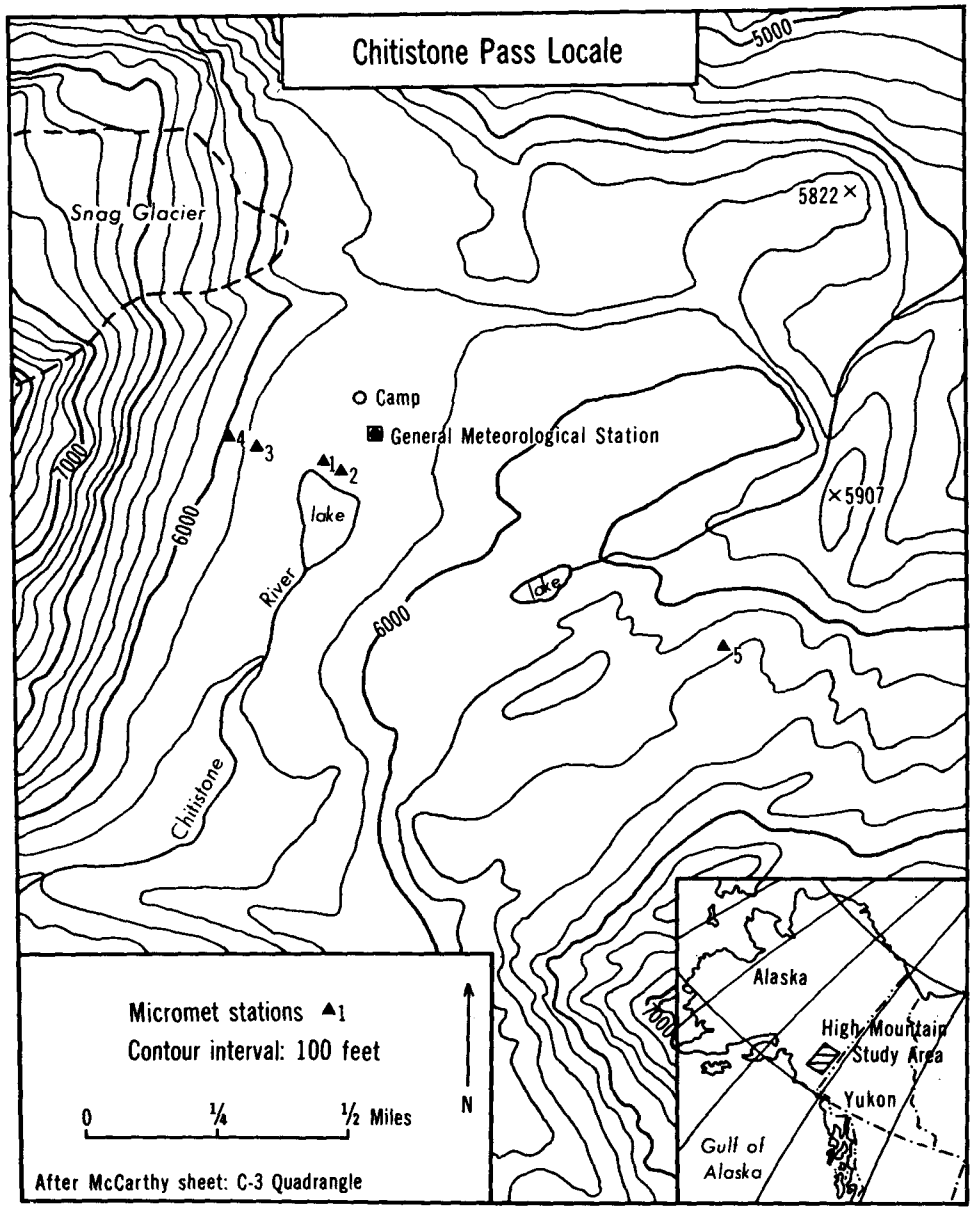

FIG. 1. Chitistone Pass locale.

2. The climate simulator

The energy transfer simulator is discussed in recent works by Outcalt (1972a, b). Thus, a full discussion of the model will not be presented. However, a general outline is given as well as the parts of the model pertaining to the assumptions inherent in calculating evaporation.

The operation of the general simulator is based on the energy conservation equation which states that the four components of the energy budget [net radiation (R_n), soil heat flux (G), sensible heat flux (H), and latent heat flux (LE)] must have a zero sum across a surface, i.e.,

$$R_n+G+H+LE=0. \quad (1)$$

Each of these terms is a complex function of the environmental variables which specify the thermal and radiative properties of the atmosphere and substrate media, and of the topographic effects at a location. At any instant in time, these components may be represented as functions of a limited set of environmental variables and physical constants. These controlling variables are listed with their notation in Table 1.

The components of the energy budget equations can

FIG. 2. Aerial photograph of Chitistone Pass area (Courtesy U. S. Geodetic Survey; 15 August 1957.) Scale 1:39,000; ▲, research station; ●, Skolai landing strip; dotted line, environmental transect.

then be written in terms of these variables and the surface temperature (T_0) as follows:

$$R_n = f(\text{LAT, DEC, } D, R, \text{ ALBEDO, } W, P, T_{\text{SKY}}, T_0, \text{SL, EX, HO}). \quad (2)$$

If the assumption is made that the soil temperature at the diurnal damping depth is approximately equal to the mean air temperature, then

$$G = f(\text{GC, GD, } T_A, T_0). \quad (3)$$

The turbulent transfer terms which are corrected for stability using the Richardson number may be expressed as

$$H = f(U, Z_0, P, T_A, T_0) \quad (4)$$

$$LE = f(U, Z_0, P, \text{RH, RHS, } T_A, T_0). \quad (5)$$

Note that in all of the above equations, after specification of the input variables, the surface temperature is the only unknown. The soil temperature profile is allowed to evolve by calculating a finite-difference solution of the thermal diffusion equation using the soil thermal solution from the preceding step. After the new

soil thermal profile is calculated, the soil heat flux is actually calculated from the uppermost soil temperature level in place of T_A.

At each step through the diurnal cycle, the solar radiation incident on a surface may be calculated for a clear day by means of a subroutine. Subroutines are also included to calculate specific humidity gradients, to fix the free air computation level, and correct the thermal properties of the atmosphere for stability.

A sequence of approximations to the surface temperature is entered into the equation for the energy exchange until the equation approaches zero. The equilibrium surface temperature is that temperature which produces a suitably small residual in the energy balance equation (e.g., 1 mly min^{-1}). Then all the components of the energy transfer regime (R_n, G, H, LE) and the soil temperature vector are retained and the next iteration begins with a forward solution of the finite-difference form of the soil thermal diffusion equation.

A detailed account of the subroutines and assumptions in the simulator is given by Outcalt (1972b). The effects of variable stratigraphy were included in an advanced version of the simulator which is used in this study, by entering a thermal diffusivity value specific to each soil computation node. The effects of site slope and exposure were evaluated using methods described

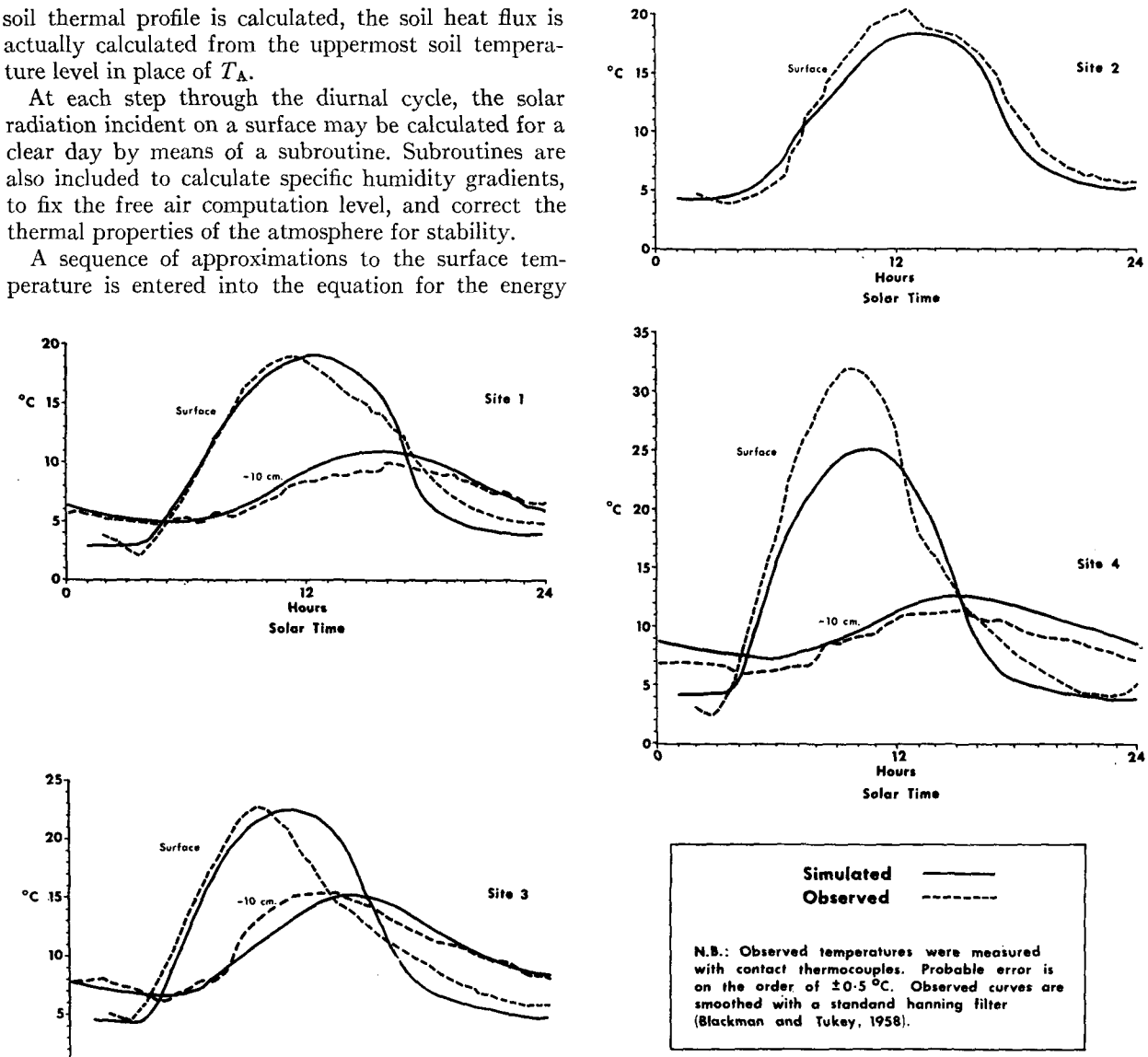

FIG. 3. Observed and simulated surface and −10 cm temperatures.

TABLE 1. Environmental input variables.

Site	Atmospheric	Soil[a]	Other
Latitude (LAT)	Mean daily air temperature (T_A)	Soil fixing depth (SD)	Elevation (E)
Date (DA)			Pressure (P)
Slope (SL)	Mean daily air relative humidity (RH)	Soil fixing temperature (ST)	Extinction coefficient (EC)
Exposure (EX)			
Roughness length (Z_0)	Mean daily wind speed (U)	Soil diffusivity (GD)	Solar declination (DEC)
Albedo (ALBEDO)		Soil volumetric heat capacity (GC)	Orbital radius vector (R)
Emissivity (E)	Mean daily precipitable Water vapor (W)		
		Soil relative humidity (RHS)	
Horizon (HO)[b]	Mean daily dust concentration (D)	Wet area fraction) (x_w)	
	Mean daily sky radiant temperature (T_{SKY})		

[a] Soil information is required for each layer within the soil: depth, diffusivity and heat capacity are specified for each soil layer.
[b] Site horizons are used every 3.75° around the compass to calculate the exposure factor.

by Gates (1962) and Kondrat'yev (1955). At each iteration, the sun elevation was tested against the horizon elevation, and the beam radiation incident at the site was weighted unity or zero, accordingly, in a manner similar to the treatment by Williams *et al.* (1972).

The details of parameter data collection are given in Brazel and Outcalt (1973). Since this paper is concerned more specifically with evaporation, the assumptions of the latent heat flux estimates in the simulator should be stated: (i) absolute humidity (q) is a function of surface temperature (T_0) only; (ii) the mean surface relative humidity (RHS) is equal to the area fraction of the immediate terrain in water or freely transpiring vegetation [an assumption originally made by Myrup (1969)]; (iii) the surface absolute humidity (q_0) is a function of the heat of evaporation (L) and the wet area fraction (x_w) as follows:

$$q_0 = (\mathrm{RHS}/L)[f(T_0)] = (x_w/L)[f(T_0)]. \quad (6)$$

(iv) the mean daily humidity is temporally constant and equal to the humidity at the air damping height. This allows a fixed humidity above, while the surface humidity fluctuates diurnally in response to the T_0 solutions to the energy balance. Thus, gradients are produced ($q - q_0$) which are used to calculate the latent heat flux.

TABLE 2. Input variables for the three sites.

Variables	Sites 1	4	5
SL (deg)	0.0	34.0	28.0
EX (deg)	0.0	125.0	315.0
Z_0 (cm)[a]	2.0	2.0	(2.0)
ALBEDO (fraction)	0.25	0.21	(0.18)
SD (cm)	55.0	150.0	150.0
GD $\times 10^4$ (cgs)	34.0	17.0	(100.0)
GC (cgs)	0.61	0.65	(0.64)
RHS (fraction)	1.00	1.00	(0.20)

Soil layers

Sites	Z (cm)	GD $\times 10^4$	GC	Description
1	0–20	34.0	0.61	organic coarse sandy gravel
	20–900	37.0	0.46	sandy clay
4	0–20	17.0	0.65	organic sandy clay
	20–900	75.0	0.46	weathered basalt
5	0–40	(100.0)	(0.64)	basalt scree
	40–900	(75.0)	(0.46)	weathered basalt

Constants for the simulation

LAT	61.6N		W	20.0
DA	(Month, day)	904 (721)[b]	D	0.20
E		0.98	T_{SKY}	−12.6C (−10.3C)
T_A		7.4C	P	835.0 mb
RH		0.81 (0.65)	ST	0.0C
U		200 cm sec^{-1} (140 cm sec^{-1})		

[a] Z_0 was estimated by calculating values from wind profiles during neutral adiabatic periods. Average daily values are used.
[b] Site 5 was not observed on 4 August, but on 21 July—a clear day also. Simulation for that day is analyzed and data used appear in parentheses above.

TABLE 3. Bowen ratios for snow-free tundra sites from selected studies.

Study	Mean daily value	Ranges	Number of days in sample
Rouse and Stewart (northern Ontario)	0.73	0.39– 1.78	19 (summer)
Rouse and Kershaw (northern Ontario)	0.61	0.26– 0.78	5 (summer)
Terjung (White Mts., Calif.)	0.30	0.19– 0.46	1 (clear day, summer)
Weller *et al.* (Barrow, Alaska)	0.12	—	4 (summer)
Mather and Thornthwaite (Barrow, Alaska)	1.81	0.08– 8.09	110 (summer)
Ahrnsbrak (central Canada)	10.00	1.81–45.14	7 (summer)
This study (southeast Alaska, Wrangell Mts.)	0.62	0.10– 1.10	11 (summer)

TABLE 4. Means of simulated and observed latent heat flux and Bowen ratios.

Site	Latent heat flux (ly min^{-1}) 24 hour Simulated[b]	24 hour Observed	Daytime[a] Simulated	Daytime[a] Observed	Bowen ratio 24 hour Simulated	24 hour Observed	Daytime[a] Simulated	Daytime[a] Observed
1	0.09	0.11	0.22	0.25	1.24	1.22	0.42	0.36
4	0.15	0.13	0.31	0.33	1.68	1.61	0.39	0.47
5	0.02	0.06	0.04	0.09	−2.69	0.08	1.86	0.91

[a] Time of significant sun exposure (for site 1, 0700–1700; site 4, 0500–1600; site 5, 1000–2100).
[b] The simulated value with the input listed in Table 2.
N.B. The simulated and observed values were for 4 August 1967 for sites 1 and 4 and 21 July 1968 for site 5. Both days were clear, calm days immediately following rainy, cloudy weather.

3. Observational methods

a. *Measurement sites*

The measurement of energy components at the three sites analyzed in this paper was conducted in August 1967 and July 1968. Observations were made at sites which are described in Table 2. The southeast-facing slope site (site 4) consisted of a continuous mat of dryas and willow vegetation. Site 1 (flat site) was typical of the flatter areas of the pass and was moss-lichen tundra. Site 5 (a northwest-facing slope) was a barren fine scree and rubble-like surface. Vegetation was very sparse.

b. *Instrumentation and measurements*

Net radiation, soil heat flux, and wet and dry bulb temperatures at two levels were observed at all three sites. Net radiation was measured by an aspirated Beckman and Whitley net radiometer placed 1 m above the surface. In the case of the sloping sites, observations had to be adjusted for shortwave radiation on slopes. An Eppley pyranometer (10-junction) was positioned at each site so as to measure both slope solar radiation and normal flat surface radiation. The difference between these two solar values was equal to the adjustment made in the observed net radiation values from the net radiometers. The probable instrument error is ±10%.

Soil heat flux was calculated by solving the equation

$$G = \mathrm{GC}\frac{\Delta T}{\Delta t}\Delta z, \tag{7}$$

where ΔT is the difference in temperature between two levels in the soil over time, Δt the time interval for the calculation, and Δz the depth difference for the calculation. Values for GC were determined periodically by analyzing partial fractions of organic, mineral and water portions of the active layer. The probable error in calculating G is ±10%.

Measurements of wet and dry bulb temperature were taken at 50 and 250 cm with an aspirated mechanical wind Assman hygrometer. Four readings were taken per hour, averaged, and the average values listed to represent on-the-hour values.

Latent heat flux was calculated using the Bowen ratio approach, i.e.,

$$LE = \frac{R_n - G}{1 + H/LE} = \frac{R_n - G}{1 + \beta}$$

$$= (R_n - G)\left[1 - \left(\frac{\gamma}{S+\gamma}\right)\left(\frac{\Delta T}{\Delta T_w}\right)\right], \tag{8}$$

where:

LE latent heat flux (ly min^{-1})
R_n net radiation
G soil heat flux
H sensible heat flux
β Bowen ratio
γ psychrometer constant [0.65 mb (°K)$^{-1}$]
S saturation vapor pressure slope
ΔT dry bulb temperature gradient
ΔT_w wet bulb temperature gradient.

The calculated Bowen ratios and latent heat fluxes from the observations were then compared with those generated from the simulations using the input and boundary conditions listed in Table 2.

4. Simulations and observations

Results of the hourly observations and simulations are given in the Appendix. Mean daily Bowen ratios were calculated for an 11-day sequence for Site 1 in 1968 (July–August). The Chitistone Pass mean values and ranges are listed in Table 3 with values cited for some other tundra sites. Tables 4 and 5 list summary data of the simulations and observations. Fig. 4 shows the comparison between simulated and observed

TABLE 5. Comparison of stimulated (th) and observed (obs) latent heat.

Site	r_{LE}[a]	Standard errors (ly min^{-1})	Regression equations
1	0.982	0.007	$LE_{obs} = -0.003 + 1.144 LE_{th}$
4	0.995	0.002	$LE_{obs} = 0.004 + 1.174 LE_{th}$
5	0.898	0.039	$LE_{obs} = -0.028 + 1.870 LE_{th}$

[a] Correlation coefficient for latent heat.

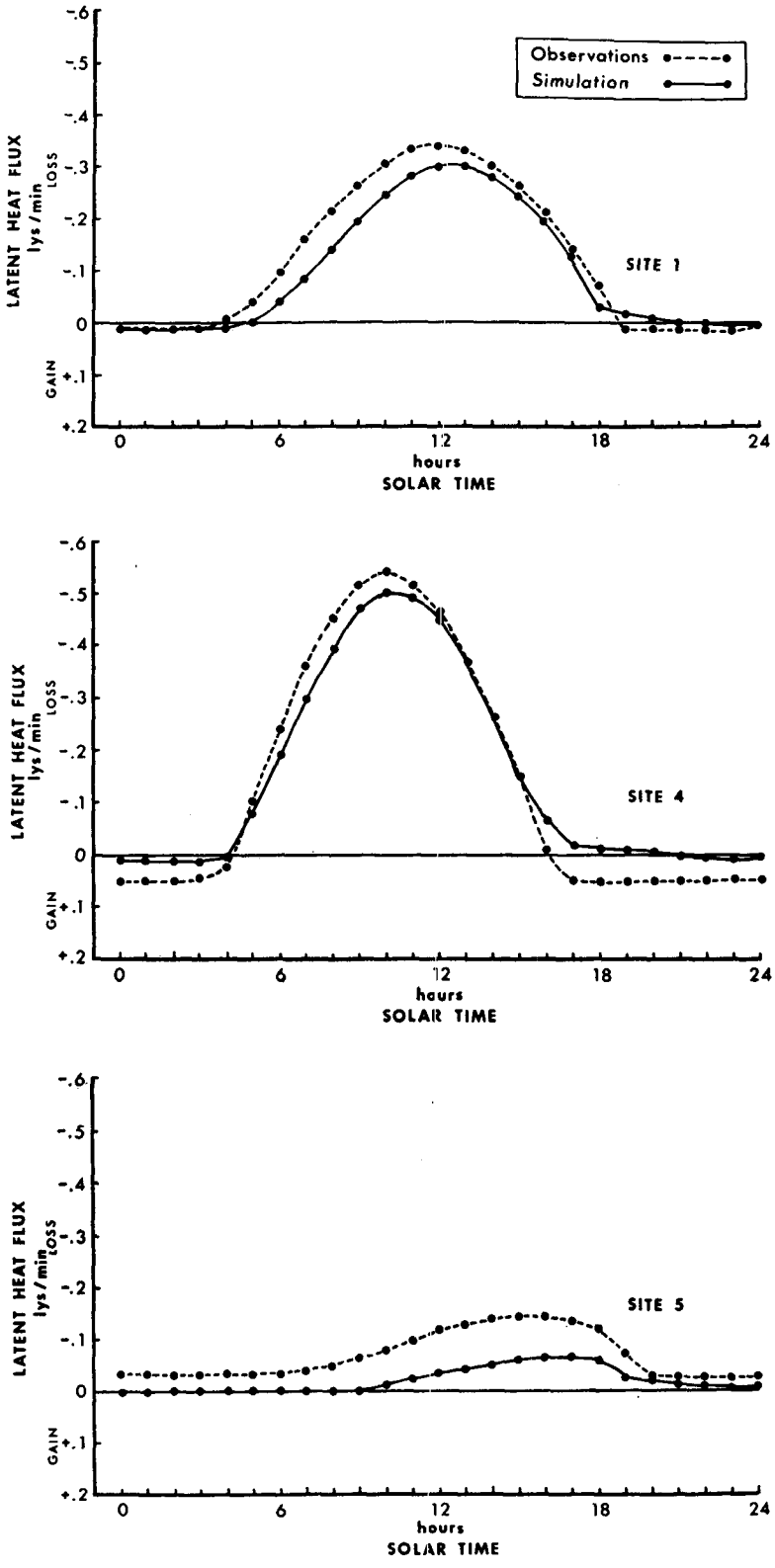

FIG. 4. Observed and simulated latent heat flux.

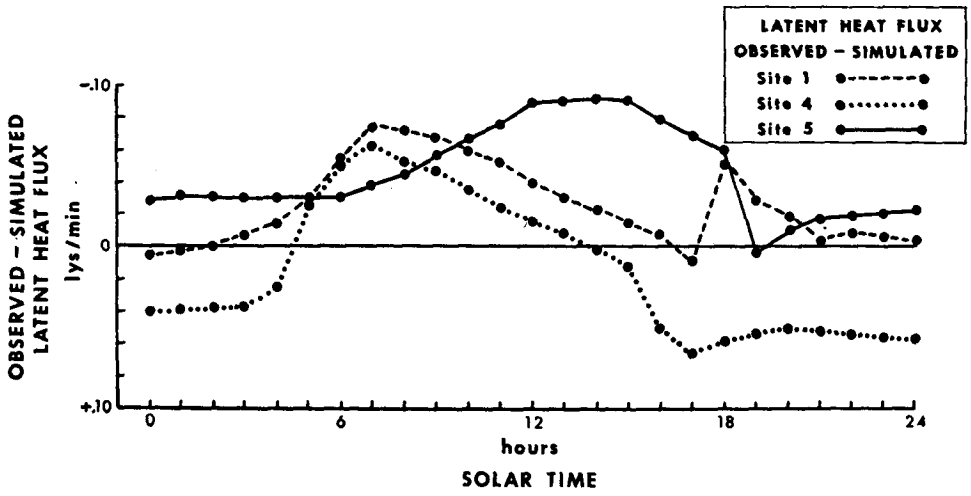

FIG. 5. Observed minus simulated latent heat flux.

evaporation, expressed in langleys per minute. Fig. 5 is a plot of the difference between simulated and observed evaporation.

There is no reason to believe that observations of R_n, G, and the Bowen ratios are any better than $\pm 10\%$. Therefore, at this stage, phase-shift and time-dependence tendencies of simulations are the only methods of comparison. In Fig. 4, amplitude and phase characteristics are similar.

For sites 1 and 4 (the vegetation-covered sites), the correlations for latent heat are very high and the standard errors very low (see Table 5). The site 5 comparison shows a weaker relationship (see Fig. 4). However, in general, the correspondence between estimates and observations is excellent (see Fig. 5). The differences between simulated and observed values do not exceed ± 0.10 ly min^{-1}, which is well within the error limit of the observations. The errors are therefore difficult to assess. The major discrepancy is for the drier site on the barren northwest-facing slope. Notice the underestimate of latent heat for that site (site 5).

Myrup (1969) has shown, for sites with wet fraction areas near 0.20, that the sensitivity of the equilibrium temperature model is very high. The chance for error in the estimates is high for sites with very low wet area fractions. This means that more divergence between estimates and observations would be expected, if wet area fraction estimates were not precisely determined. This probably is the case in this study. Site 5, on the drier slopes, consisted of scree and rubble, but the entire northwest slope had many benches where standing water existed. Also, the vegetation cover tended to be more continuous on these benches. The immediate slope where the instrument complex was located was virtually devoid of vegetation and standing water at the surface. As a result, the assigned estimate of 0.20 for wet fraction is perhaps too low (underestimating latent heat and overestimating Bowen ratios in the simulations).

For dry sites, a very accurate estimate of wet area fraction is needed to more fully test the model. Sites 1 and 4, which were sites of continuous vegetation, are estimated to a much higher degree, since $x_w \rightarrow 1.0$. Further, these latter two sites were near field capacity throughout both field seasons. This general area, near the Gulf of Alaska, is one of the most humid regions of the Pacific Littoral.

The fact that the sites never really experienced much of a drying cycle probably accounts for the very high correlation with the simple model estimates. Sites of "moderate dryness," such as that in the study of Rouse and Stewart (1972), and site 5 in this study, cause divergence in the equilibrium theory model unless the wet area fraction and the assumption inherent in it can be accurately assessed.

The employment of the wet area fraction concept is a matter of convenience. Further work is necessary to relate the soil moisture conditions to this parameter. In this study, no detailed water budget information was collected for these sites. However, to enhance further the simulation approach, it is necessary to couple the heat and mass transfer regimes in an approach similar to that of Kennedy and Lielmezs (1973).

5. Conclusion

Evaporation and Bowen ratio observations, and their variation during high solar radiation conditions across an alpine tundra landscape, agree favorably with estimates produced by an equilibrium temperature model described by Outcalt (1972a). Brazel and Outcalt (1973) have shown that thermal contrast in the tundra is predictable using this model (see Fig. 3). It is expected that for an equilibrium solution, the components of the energy budget should be correct when there is good convergence with measured surface temperature. This paper confirms this expectation except for drier sites. In portions of the terrain where vegetation is continuous, evaporation estimates are predictable

using the model. In an environment where the tundra never experiences desiccation, the simple equilibrium model assumptions concerning the wet area fraction are not restricting. Most alpine pass environments along the Pacific Littoral are high moisture environments, so that the model may be applicable to several of these areas. The model is capable of reproducing spatial contrast in energy components across the highly variable tundra terrain.

6. Future research

Further cooperative research work between climatologists at the Universities of Windsor and Michigan is planned in which the equilibrium temperature solution will be forced by high-frequency measurements (15 min) of air temperature, humidity and wind velocity at screen height. The initial observation series will probably have to be filtered to remove high frequencies. A turbulent flux model subroutine modified by Goodwin (1972), from a program developed by Ryznar (1971) using the Businger-Dyer model (Businger, 1966), should eventually make possible field energy budget studies using measurements from one level in the atmosphere and surface thermal regime measurements in conjunction with high-frequency solar radiation data.

Acknowledgments. The authors wish to express thanks to those responsible for making this study possible. The Arctic Institute of North America and the Army Research Office (Durham, N.C.) sponsored the research and provided logistical support to the High Mountain Environment Project (Marcus, 1971). Several individuals assisted Dr. Brazel in field collection of energy balance data. Thanks are extended to W. Benjey, B. Bishop, F. Dumoy, J. Ford, J. Hallorin, S. Loomis, D. Porter, D. Scott and J. Willingham. Dr. Melvin G. Marcus of the Department of Geography, University of Michigan, led the field research phase of this study. Dr. Outcalt performed the numerical modelling used in this analysis. The simulation program was written at the Department of Geography by Dr. Outcalt and modified by his graduate students, A. Terroux and C. Goodwin. Interested parties may obtain a source code listing by writing Dr. S. I. Outcalt, Department of Geography, University of Michigan, Ann Arbor, Mich. 48104.

APPENDIX

Simulations and Observations of Bowen Ratios and Latent Heat Flux

	Bowen ratios			Latent heat flux		
	Site			Site		
Time	1	4	5	1	4	5
			A. Simulations			
00	3.58	4.44	−4.50	0.012	0.009	−0.004
01	3.38	3.81	−11.00	0.013	0.011	−0.002
02	3.00	3.58	−12.50	0.015	0.012	−0.002
03	2.93	3.58	−28.00	0.016	0.012	−0.001
04	3.21	33.00	−30.00	0.014	0.001	−0.001
05	−5.60	0.32	—	−0.005	−0.079	0.000
06	−0.02	0.44	—	−0.040	−0.186	0.000
07	0.34	0.43	16.50	−0.086	−0.298	0.002
08	0.43	0.41	−12.50	−0.139	−0.399	−0.002
09	0.44	0.39	−2.00	−0.194	−0.471	−0.005
10	0.42	0.38	1.00	−0.242	−0.505	−0.011
11	0.43	0.40	1.84	−0.278	−0.495	−0.019
12	0.43	0.40	2.17	−0.297	−0.445	−0.028
13	0.43	0.42	2.26	−0.296	−0.363	−0.038
14	0.43	0.44	2.22	−0.276	−0.262	−0.046
15	0.44	0.44	2.17	−0.240	−0.156	−0.057
16	0.44	0.23	2.16	−0.192	−0.063	−0.062
17	0.43	−1.18	2.17	−0.139	−0.016	−0.062
18	−0.71	−2.66	2.19	−0.021	−0.009	−0.057
19	−2.30	−5.60	2.04	−0.010	−0.005	−0.023
20	−7.25	−31.00	1.50	−0.004	−0.001	−0.014
21	11.33	11.66	0.60	0.013	0.003	−0.010
22	6.33	7.40	−0.50	0.006	0.005	−0.007
23	4.44	5.42	−1.66	0.009	0.007	−0.006
24	4.10	4.87	−3.50	0.010	0.008	−0.004
			B. Observations			
00	2.86	0.80	−0.60	0.015	0.050	−0.030
01	2.93	0.84	−0.73	0.015	0.050	−0.030
02	3.00	0.86	−0.83	0.015	0.050	−0.030
03	4.70	0.86	−0.93	0.010	0.050	−0.030
04	—	1.32	−1.00	0.000	0.025	−0.030
05	−0.82	0.25	−1.03	−0.034	−0.105	−0.030
06	−0.01	0.35	−1.10	−0.095	−0.240	−0.030
07	0.19	0.36	−0.94	−0.160	−0.360	−0.035
08	0.29	0.36	−0.55	−0.210	−0.450	−0.045
09	0.33	0.36	−0.17	−0.260	−0.518	−0.060
10	0.36	0.36	0.15	−0.300	−0.540	−0.075
11	0.37	0.37	0.37	−0.330	−0.518	−0.095
12	0.39	0.39	0.53	−0.335	−0.460	−0.115
13	0.40	0.41	0.69	−0.325	−0.370	−0.125
14	0.41	0.45	0.79	−0.298	−0.260	−0.135
15	0.42	0.48	0.86	−0.254	−0.145	−0.140
16	0.43	1.50	0.96	−0.200	−0.010	−0.140
17	0.46	0.38	1.04	−0.130	0.050	−0.130
18	−0.21	0.48	1.09	−0.070	0.050	−0.115
19	1.53	0.56	3.10	0.015	0.050	−0.020
20	1.93	0.62	1.04	0.015	0.050	−0.025
21	2.67	0.70	0.36	0.015	0.050	−0.025
22	2.53	0.74	−0.04	0.015	0.050	−0.025
23	2.60	0.76	−0.40	0.015	0.050	−0.025
24	2.73	0.78	−0.56	0.005	0.050	−0.025

REFERENCES

Ahrnsbrak, W., 1968: Summertime radiation balance and energy budget of the Canadian tundra. Tech. Rept. 37, Dept. of Meteorology, University of Wisconsin.

Blackman, R. B., and J. W. Tukey, 1958: *The Measurement of Power Spectra.* New York, Dover, 190 pp.

Bowen, I., 1926: The ratio of heat losses by conduction and by evaporation from any water surface. *Phys. Rev.*, **27**, 779–787.

Brazel, A., and S. Outcalt, 1973: The observation and simulation of diurnal surface thermal contrast in an Alaskan alpine pass. *Archiv. Geophys., Meteor. Bioklim.*, (in press).

Brunt, D., 1934: *Physical and Dynamical Meteorology*. Cambridge University Press, 428 pp.

Businger, J. A., 1966: Transfer of momentum and heat in the planetary boundary layer. *Proc. Symp. Arctic Heat Budget and Atmospheric Circulation*, RM-5233-NSF, Rand Corp., 305 pp.

Gates, D., 1962: *Energy Exchange in the Biosphere*. New York, Harper and Row, 151 pp.

Goodwin, C. W., 1972: An annual active-layer simulator for permafrost regions. M.Sc. thesis, University of Michigan.

Kennedy, G. F., and J. Lielmezs, 1973: Heat and mass transfer of freezing water-soil system. *Water Resources Res.*, **9**, 395–400.

Kondrat'yev, Y., 1955: *Radiative Heat Exchange in the Atmosphere*. Pergamon Press (transl. by O. Tedder, Oxford).

Lettau, H., 1951: Theory of surface-temperature and heat-transfer oscillations near a level ground surface. *Trans. Amer. Geophys. Union*, **32**, 189–200.

Lonnqvist, O., 1962: On the diurnal variation of surface temperature. *Tellus*, **14**, 96–101.

——, 1963: Further aspects on the diurnal temperature variation at the surface of the earth. *Tellus*, **15**, 75–81.

Marcus, M., 1971: The High Mountain Environment Project: St. Elias Mountains, Yukon and Alaska 1967–1971. Res. Paper No. 61, Arctic Institute of North America, Washington, D. C.

Myrup, L., 1969: A numerical model of the urban heat island. *J. Appl. Meteor.*, **8**, 908–918.

Outcalt, S., 1972a: The development and application of a simple digital surface-climate simulator. *J. Appl. Meteor.*, **11**, 629–636.

——, 1972b: The simulation of subsurface effects on the diurnal surface thermal regime in cold regions. *Arctic*, **25**, 305–307.

Rouse, W. R., and K. A. Kershaw, 1971: The effects of burning on the heat and water regimes of lichen-dominated subarctic surfaces. *Arctic Alpine Res.*, **3**, 291–304.

——, and R. Stewart, 1972: A simple model for determining evaporation from high-latitude upland sites. *J. Appl. Meteor.*, **11**, 1063–1070.

Ryznar, E., 1971: Wind and temperature structure in the surface layer of the atmosphere. Rept. 08653-1-F, Contract DAGCO 4-67-C-0027, USARO, University of Michigan.

Scott, R., 1971: Ecology and phytogeography of alpine vegetation in the southeastern Wrangell Mountains, Alaska. Ph.D. dissertation, University of Michigan, 314 pp.

Terjung, W., 1969: Energy and moisture balance of an alpine tundra in mid-July. *Arctic Alpine Res.*, **1**, 247–266.

Weller, G., *et al.*, 1972: The tundra microclimate during snowmelt at Barrow, Alaska. *Arctic*, **25**, 291–300.

Williams, L. D., R. G. Barry and J. T. Andrews, 1972: Application of computed global radiation for areas of high relief. *J. Appl. Meteor.*, **11**, 526–533.